

Array Beamforming Response Studies

GEORGE W. BYRAM, GEORGE V. OLDS
AND LEON P. LALUMIERE

*Signal Processing Branch
Acoustics Division*

October 14, 1971

PLEASE RETURN THIS COPY TO:

NAVAL RESEARCH LABORATORY
WASHINGTON, D.C. 20390
ATTN: CODE 2028

Because of our limited supply you are requested to return this copy as soon as it has served your purposes so that it may be made available to others for reference use. Your cooperation will be appreciated.

NDW-NRL - 5070/2035 (10-67)



NAVAL RESEARCH LABORATORY
Washington, D.C.

CONTENTS

Abstract	ii
Problem Status	ii
Authorization	ii
INTRODUCTION	1
AMPLITUDE SHADING	2
WAVEFRONT CURVATURE AND ARRAY FOCUSING	3
FREQUENCY RESPONSE AND SPATIAL SAMPLING	6
SIDE-LOBE DEPENDENCE ON STEERED BEAM DIRECTION	6
LINEAR-ARRAY PATTERN EXTRAPOLATION	9
PLANAR AND VOLUME ARRAYS	12
USE OF COMPUTER PLOTS IN ARRAY STUDY	17
REFERENCES	19

ABSTRACT

Computer graphics have been used to display the results of array beamformer computations in a form aiding insight into beamforming characteristics. In particular, the effect of a parameter such as frequency, wavefront curvature, beam angle, or shading on array response can be easily seen. The examples are chosen to illustrate those characteristics as well as to aid insight into a number of important array properties. The associated theory is briefly summarized with each example, and the emphasis on important array properties makes the report useful as a tutorial review.

PROBLEM STATUS

This is a final report on one phase of a continuing problem.

AUTHORIZATION

NRL Problem S01-39
Project RF 05-552-403-4069

Manuscript submitted July 22, 1971.

ARRAY BEAMFORMING RESPONSE STUDIES

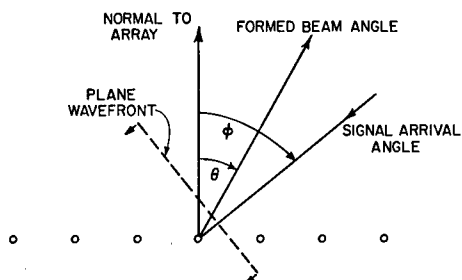
INTRODUCTION

The majority of sonar systems as well as some radio and radar systems use a beam-formed array as their primary sensor. An array of small receptors is the most convenient means of sampling an extended field. It is often the only feasible means in large-scale, long-wavelength applications such as sonar.

Since the individual receptors of a large array cannot be moved, control of the array directional sensitivity must be introduced through processing of their output signals. The beamformer performs this task by altering the relative delays and amplitudes of individual receptor outputs before summing them to form an array output.

The basic geometric variables involved in array response are shown in Fig. 1. The special case of a linear array has been chosen for simplicity. Even in the more general case of a planar or volume array, only two main directions will be of interest. These are the actual direction of signal arrival and the desired, or beamformed, direction. Signals are assumed to be plane waves normal to the chosen direction (except for one case to specifically test the effect of wavefront curvature). In addition, isotropic elements of ideal response and with uniform illumination and regular arrival times are hypothesized.

Fig. 1 - Geometric variables involved in the response of a linear array of ideal isotropic elements with uniform illumination. Formed beam angle θ is measured from the normal to the array; the plane wavefront is moving in a direction at an angle ϕ to the normal.



The combined effect of the array and the beamformer can be approximated quite closely by the equivalent circuit of Fig. 2. In this circuit the delays on the right represent actual delay operations in the beamformer. The delays on the left represent differences in propagation delay to the individual receptors. The delays in the beamformer compensate for the differences in propagation delay for signals arriving from the beamformed direction, so that the total delay in each channel is the same. The parallel combination of equal delays then is equivalent to a single delay. If additional channels are provided in the beamformer, separate outputs corresponding to different beamformed directions can be derived.

The equivalent circuit for directions other than the beamformed direction is a parallel combination of unequal delays. The response of such a network is strongly frequency dependent. Since the beamformer delays depend on the desired reception direction and the propagation delays depend on the actual direction of signal arrival, the directional response and the frequency response are inherently coupled. The weights shown in Fig. 2, which provide for adjustment of gains of individual elements, are used to shade the array to help control side-lobe response.

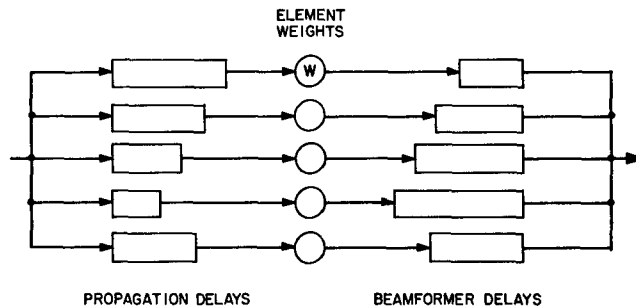


Fig. 2 - Equivalent circuit of the beamformed array illustrating the beamforming procedure. Propagation delays are due to the medium; compensating delays are inserted and adjusted to form the beam in the desired direction. Side lobes are reduced by weighting the relative strength of individual elements.

The response of an array-beamformer combination can be computed quite easily on the basis of the equivalent circuit. The large number of parameters involved, however, complicates the interpretation of numerical results. The use of three-dimensional computer plotting techniques permits display of the response in a form which shows the influence of a parameter directly. This method greatly aids insight into array properties.

Most of the remainder of this report consists of examples chosen to illustrate the application of plotting techniques to array study. The associated array theory is described briefly with each example. These examples provide a convenient tutorial overview of important array properties. A final section provides some guidelines for setting up problems to be studied by these methods. The computer programs used for most of this work are available (1-3).

AMPLITUDE SHADING

Amplitude shading of an array permits a tradeoff between main-lobe width and side-lobe amplitude. The same process is known as apodization in optics and as instrument profile adjustment in spectroscopy. An extensive body of literature exists on the design of optimum shading functions (4). As a useful generalization, however, a concentration of sensitivity near the center of an instrument aperture combined with a smooth taper toward the extremes reduces side lobes. A concentration of sensitivity in the extremes of the aperture improves angular resolution at the expense of increased side lobes. A telescope with a central obstruction may resolve closely spaced double stars but exhibit low contrast on extended objects, due to the bright outer rings in its diffraction pattern.

An array-shading scheme which optimizes tradeoff between main-lobe width and side-lobe level, by giving the minimum main-lobe width between first nulls for a specified main-beam-to-side-lobe ratio (or the converse, minimum side-lobe amplitude for a given main-lobe width), and which also results in equal-amplitude side lobes is the Dolph-Tchebyscheff weighting (5). Figure 3 shows the broadside response of such an array as a function of the design peak-to-side-lobe ratio. The plot covers a wider range of cases than would be encountered in practice. The back of the plot corresponds to the limiting case of an edge array in which only the end elements are used. In that case, which is analogous to an interferometer, the side lobes are as strong as the main lobe. The front of the plot corresponds to a 45-dB peak-to-side-lobe ratio. An infinite peak-to-side-lobe ratio would correspond to a set of weights proportional to binomial coefficients. This also is a limiting

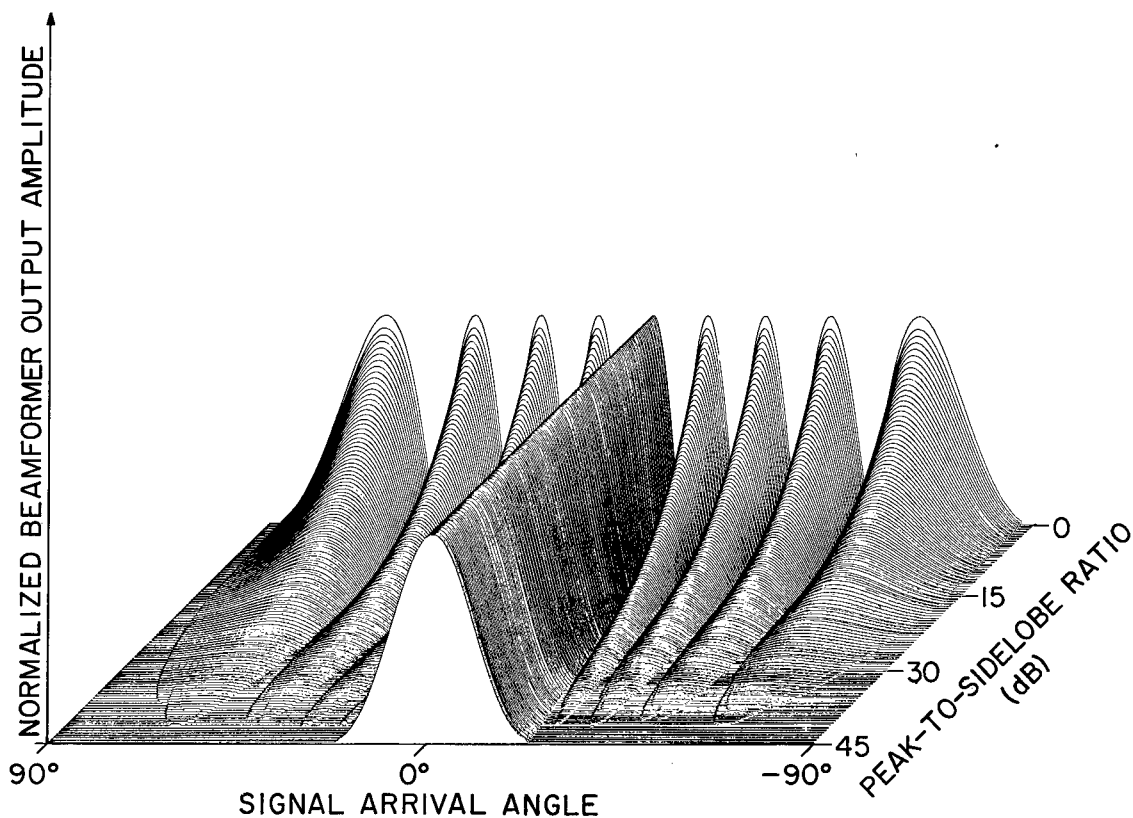


Fig. 3 - Response of ten element, equispaced array beamformed broadside. Spacing between the elements is 0.5 wavelength. Response is shown for Dolph-Tchebyscheff shadings for peak-to-side-lobe ratios ranging from -45 dB to 0 dB in 0.25-dB steps.

case of the Dolph-Tchebyscheff array. The increased width of the main lobe with more severe shading is visible as a broadening of the main lobe near the front of the plot.

For the case shown in Fig. 3 the beamformer delays were all equal, since broadside arrivals reach all receptors simultaneously. Figure 4 shows the effect of introducing delays to favor arrivals 45° to broadside.

WAVEFRONT CURVATURE AND ARRAY FOCUSING

The computations for Figs. 3 and 4 assumed a plane wavefront. If a source is quite close to the array, however, the curvature of the wavefront can be significant. In some cases it is possible to focus the array to favor a specific range.

Two arrays are shown in Fig. 5. Both are 3.5 wavelengths long, and each is focused on a point 5 wavelengths from its center. This is an extreme case which would not be encountered in sonar. The linear array is focused by adding extra delay in the beamformer for the inner elements. The curved array has been focused by bending it to match the curvature of the desired wavefront. Figure 6 compares the response of these two arrays. The response patterns are almost identical. The fast rise to maximum response and the slow fall-off as range exceeds the focal distance are typical of most cases. Effects near and beyond the focal distance are less noticeable for greater focal distances.

Figure 7 shows the degradation in response of a linear array as the range becomes much less than the focal distance. For extremely small ranges the main lobe is greatly reduced, but there is only a slight increase in side-lobe level. This is to be expected, since

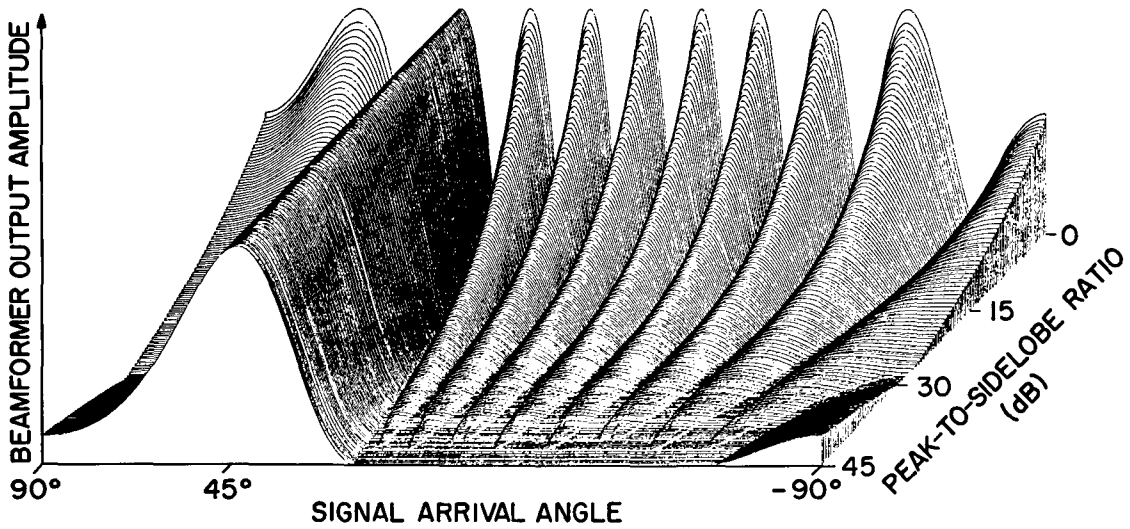


Fig. 4 - Response of the same array as in Fig. 3 except that the beam is formed at 45°

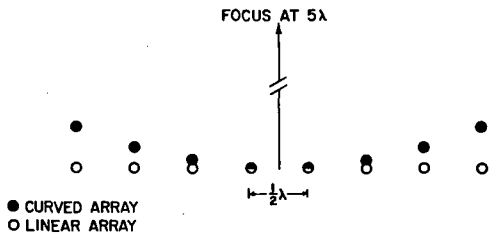


Fig. 5 - Comparison of an eight-element array curved to focus at 5 wavelengths with the linear array requiring delays adjusted to compensate for the same wavefront curvature

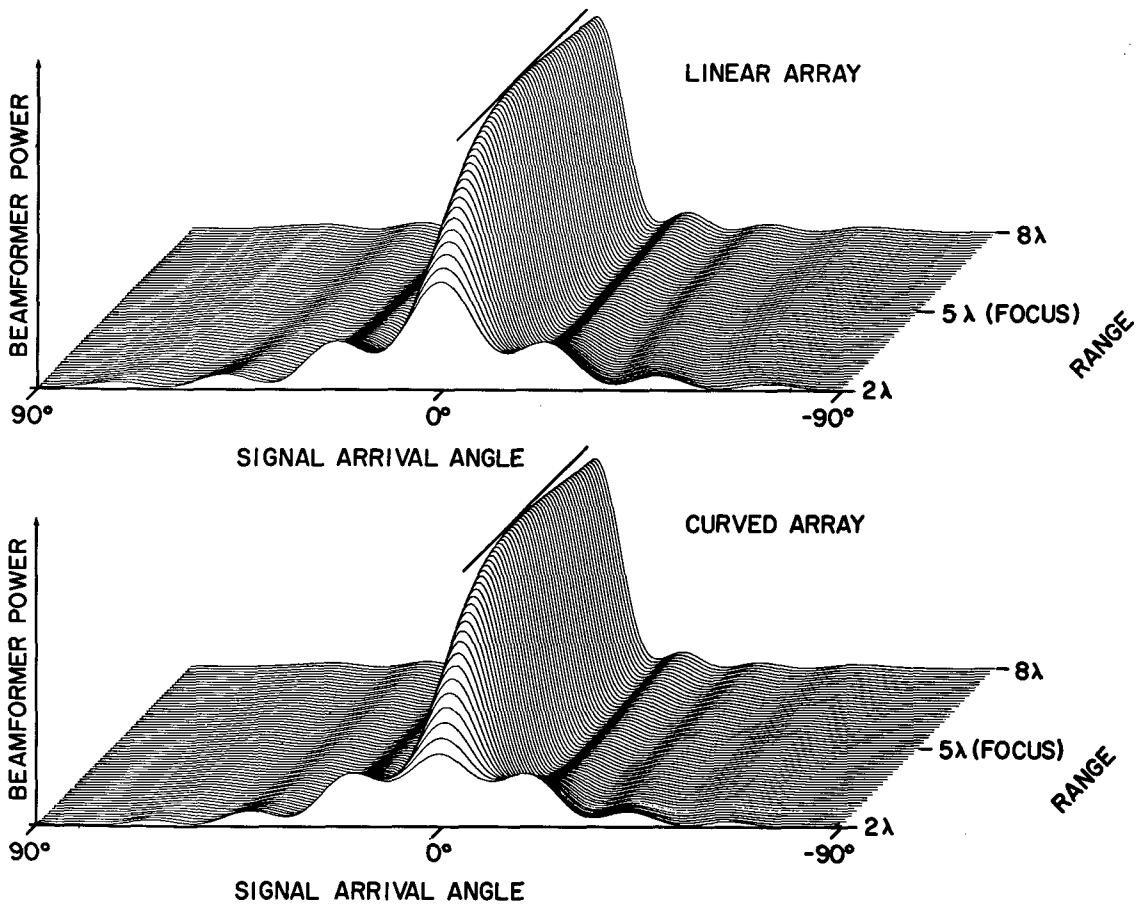


Fig. 6 - Response of the two arrays of Fig. 5 with range to the point source varying from 2 to 8 wavelengths and with the beam formed at 0°

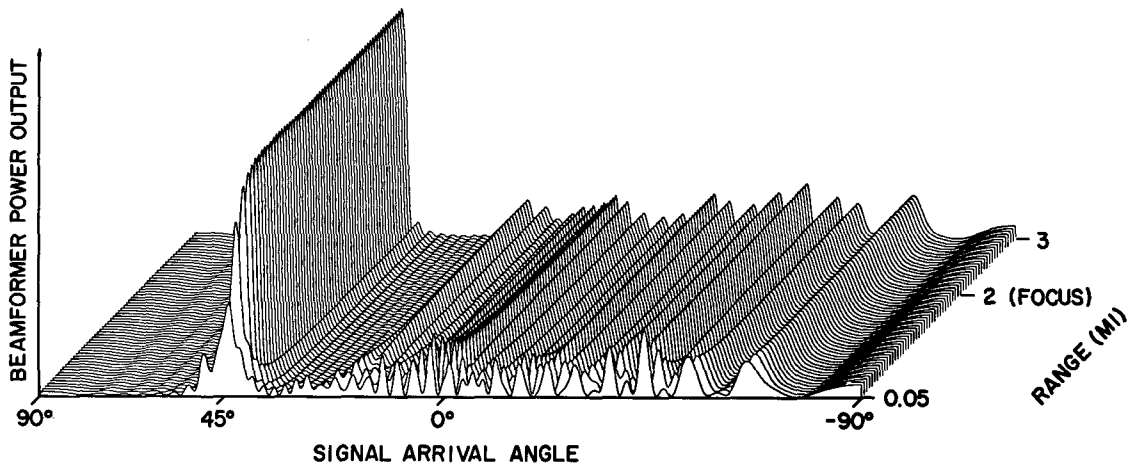


Fig. 7 - Response of a 14-element, linear array with an element spacing of $(3\lambda/2)(1.1)^{n-1}$ for each n th space from the end. The delays are adjusted to form the beam at 45° for a curved wavefront of 2-miles radius. The plot shows degradation of the response as the actual range of the signal source is reduced.

the phase errors resulting from wavefront curvature are no worse than those already existing for signals arriving from nonbeamformed directions.

The extremely small delay differences involved in focusing an array at any reasonable distance would be lost in the delay fluctuations caused by local propagation effects. Hence the pattern degradation at small ranges is the most significant result shown in Fig. 7. The very weak dependence of the pattern on range and focal distance for larger values indicates that the plane-wave assumption is justified in almost all practical cases.

FREQUENCY RESPONSE AND SPATIAL SAMPLING

A minimum length for an array is often dictated by a specified maximum width for its main lobe. If the number of receptors is limited, their spacing may be greater than a half wavelength, and the array will be undersampled. Strong grating lobes will be present if the elements are equally spaced. These lobes arise from a cycle-to-cycle ambiguity. Figure 8 illustrates the process for the simple case of a linear array steered broadside. At twice the frequency shown, ambiguity would occur every other cycle in the directions shown, and single-cycle ambiguity would occur in some directions more nearly normal to the array. The problem is less severe if the signal has high bandwidth or if the array has nonuniform spacing. A periodic, undersampled array does not gather sufficient independent information to permit unique determination of the direction of arrival of a low-bandwidth signal.

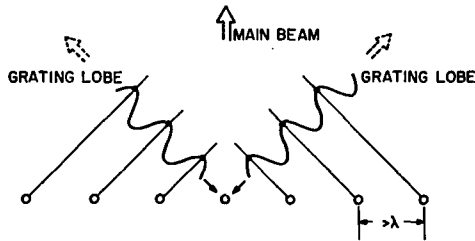


Fig. 8 - Grating lobes caused by cycle-to-cycle ambiguity. Undersampling results from the element spacing exceeding 0.5λ (equivalent of Nyquist interval for spatial sampling). The main beam is indistinguishable by the summing process from the indicated side lobes.

The frequency dependence of the response of a 14-element, equispaced array is shown in Fig. 9. The element spacing in this array is a half wavelength at approximately 500 Hz. Hence there are two grating lobes at 1 kHz and four at 2 kHz. If the spacing is perturbed to disrupt the periodicity, the grating lobes will be spread into many smaller lobes. Figure 10 shows the result of adding linearly increasing multiples of ten percent to the spacings, starting at one end. The array is now more severely undersampled, but the largest side lobe is 5 or 6 dB down from the main lobe. The reduced width of the main lobe results from the increased length of the array. The side-lobe reduction would have been slightly improved if the perturbed spacing had been rescaled to the same total length as the equispaced array. For a fixed length and a fixed number of elements, a point of diminishing returns is reached quite rapidly, and extensive search for optimum spacing schemes yields only slight further improvement.

Two other interesting relationships are apparent in Fig. 10. First, the response is frequency invariant only in the formed beam direction. Any slice through the response surface for a constant direction of signal arrival is a frequency-response plot in that direction. Second, the height of any given side lobe remains constant. Only its distribution in frequency and signal arrival angle changes.

SIDE-LOBE DEPENDENCE ON STEERED BEAM DIRECTION

A steered-beam direction of 45° was used for the plots of Figs. 9 and 10. This choice helped avoid hiding side-lobe detail behind the ridge corresponding to the main lobe. To

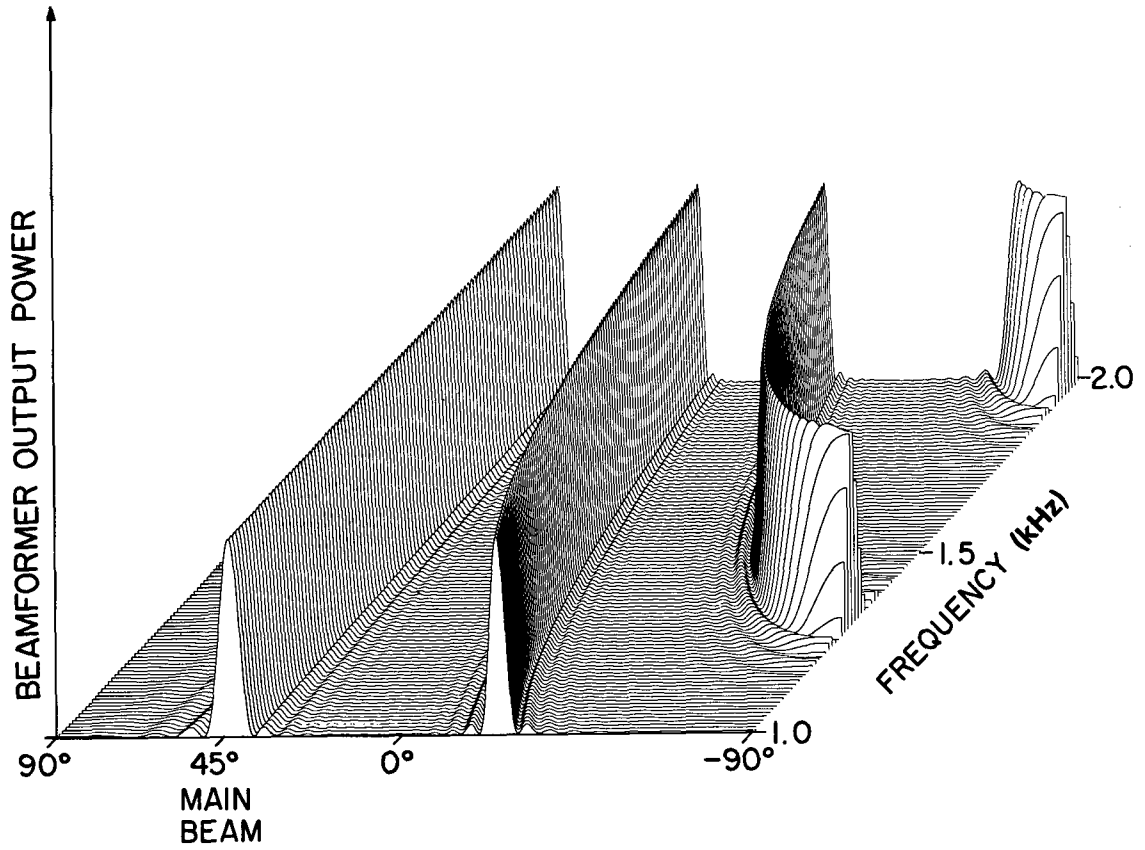


Fig. 9 - Variation with frequency of the response of a 14-element, equispaced, unshaded array. The beam is formed at 45°, and the spacing is 1 wavelength at 1 kHz.

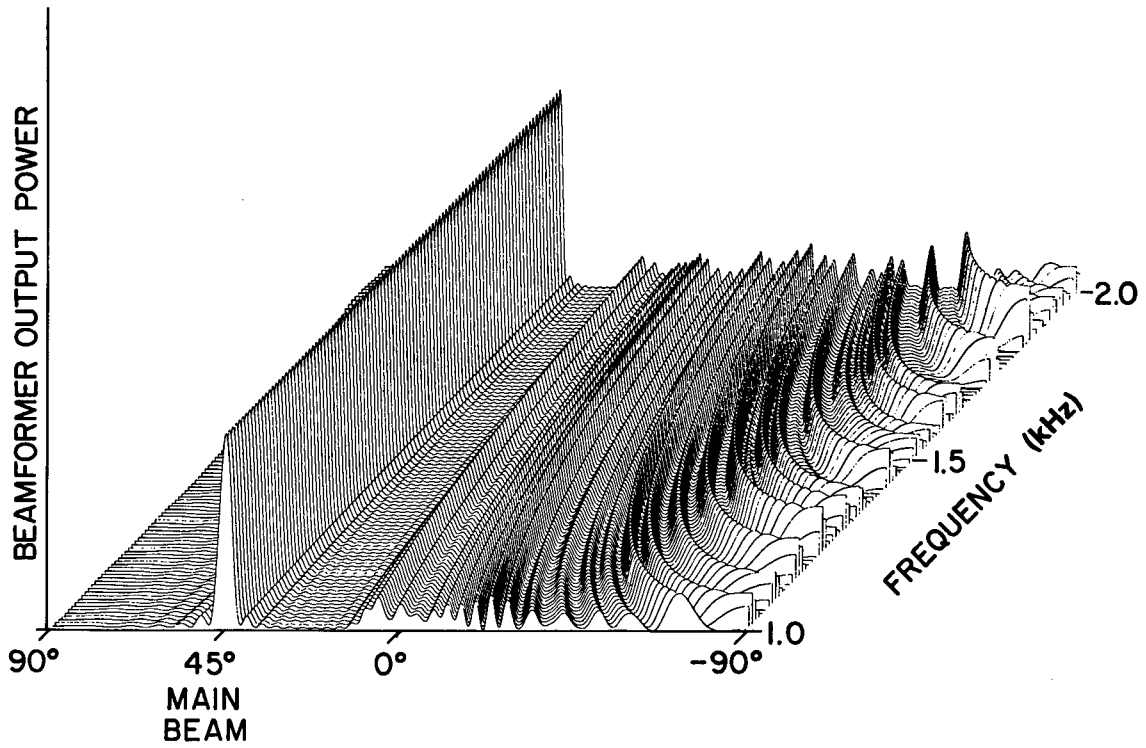


Fig. 10 - Response of a perturbed array having the same parameters as in Fig. 9 except that each n th space from the end is $(1.1)^{n-1}$ wavelength long at 1 kHz.

show the influence of main-beam steering angle on side-lobe structure, beam angle can be used as the third variable for a fixed frequency. Figure 11 shows the beam-angle dependence of the array of Fig. 10 at a frequency of 1.5 kHz. The height of any given side lobe remains constant, as shown in Fig. 10, but its distribution in the signal-angle/beam-angle plane changes. The broadening of the main lobe near the two endfire directions in Fig. 11 is a diffraction effect arising from the smaller effective aperture which the array presents to an oblique arrival. This same broadening is visible in the side lobes in both the frequency-response and the beam-dependence plots.

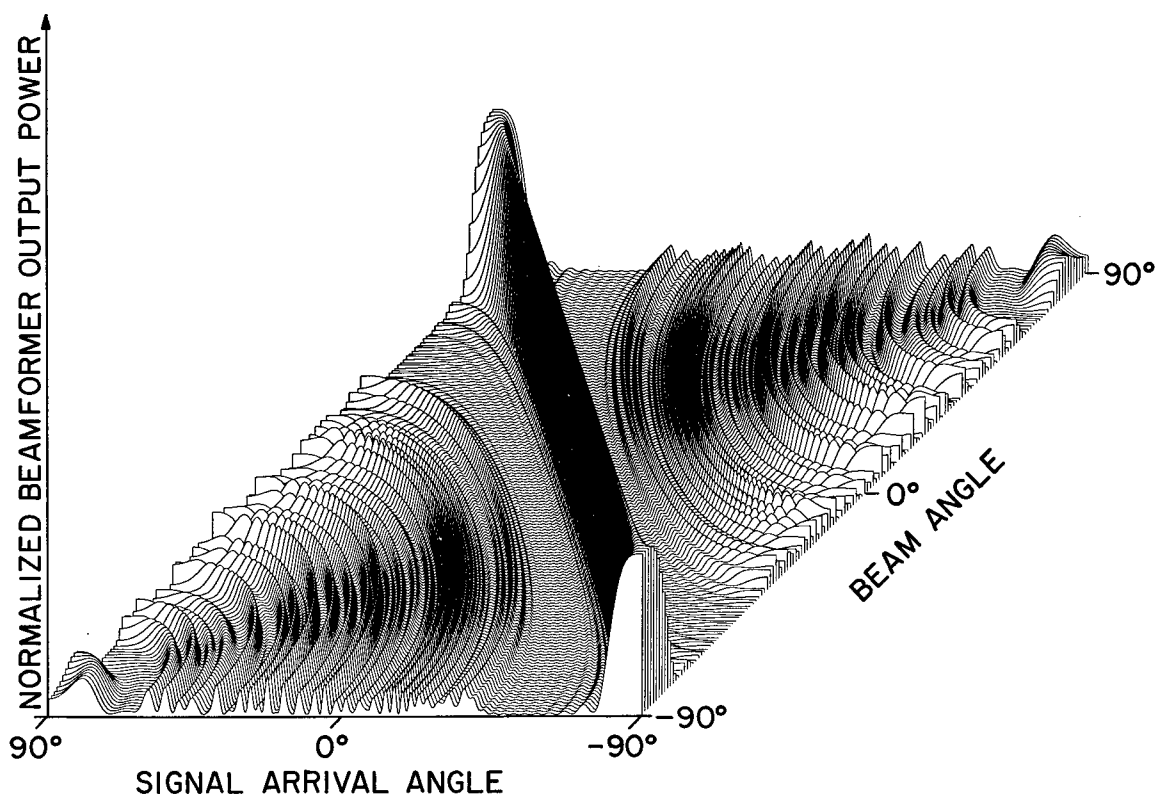


Fig. 11 - Beam-angle dependence of the response of the array of Fig. 10 at 1.5 kHz

The same 1.5-kHz slice of Fig. 10 used in Fig. 11 was also used for the wavefront curvature plot of Fig. 7.

LINEAR-ARRAY PATTERN EXTRAPOLATION

The constant amplitude of individual side lobes in the frequency-response and beam-dependence plots suggests a closer look at the theory. The array response is dependent on the spatial frequency it observes. This depends on frequency, signal arrival angle, and the velocity of sound. The beamformer modifies the response by adding extra delays dependent on the desired beam direction. Hence frequency, beam direction, and signal arrival angle occur only in fixed combination in the array-response equations. If one of these three variables is held constant, then constant values of this combination correspond to contours of constant amplitude in the plane defined by the other two variables. For a linear array under the conditions previously stated, contours of constant amplitude in the frequency-response plots follow the family of curves defined by the equation

$$f = \frac{\text{constant}}{\sin \phi - \sin \theta} \Big|_{\theta \text{ fixed}}$$

where f is frequency, θ is beam steering angle, and ϕ is signal arrival angle. Similarly, contours of constant amplitude in the beam-dependence plots follow the family of curves defined by the equation

$$\theta = \sin^{-1} (\text{constant} + \sin \phi) \Big|_{f \text{ fixed}}$$

These equations are independent of the number, spacing, and amplitude weighting of elements in a linear array. Hence plots of these equations are useful for extrapolation of array patterns. They permit a large amount of information to be derived from a single known pattern.

The beam-angle extrapolation curves are shown in Fig. 12. These curves could have been linearized by removing the sine dependence in θ and ϕ . Preserving this dependence, however, permits direct use of the curves as an overlay on conventional pattern plots. The curves are plotted for 3° increments for θ at the intersection of a diagonal with the contours. The contours show how any selected level of response on a known pattern will vary as the formed beam direction is changed. Entry to the chart for the known pattern is on the horizontal line corresponding to its beam angle. Features of interest, for example large side lobes, can then be followed along the curves to the line corresponding to the new beam angle and the shift in direction of the signal producing the side lobe thereby determined. For example, one may assume a strong side lobe is created by a signal arriving at $\phi_1 \approx 66^\circ$ for a main beam formed at $\theta_1 = 45^\circ$. The same amplitude lobe would appear at a signal arrival angle of $\phi_2 \approx 45^\circ$ for a beam formed at $\theta_2 = 30^\circ$. For more detailed extrapolation a complete pattern could be drawn for the new beam direction of interest, or a new scale could be prepared for the original direction.

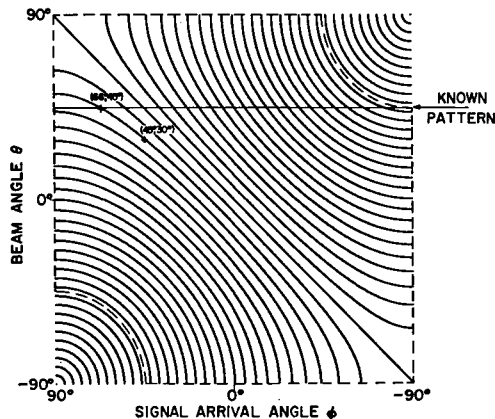
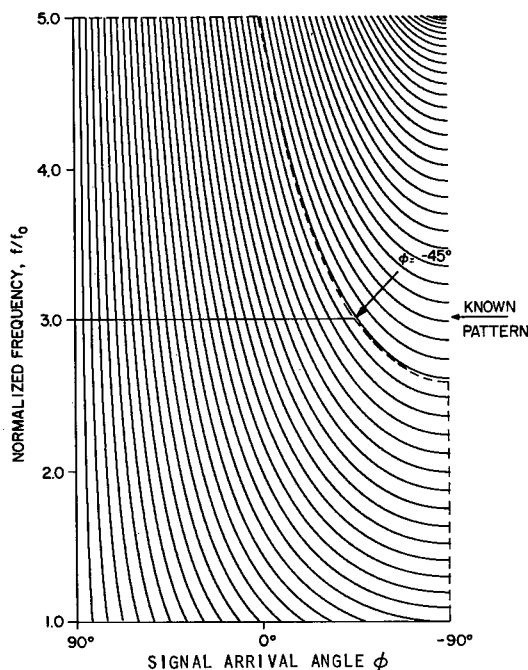


Fig. 12 - Contours of constant amplitude for any response pattern of a linear array at a given frequency. The contours illustrate the relationship between side-lobe structure and formed beam angle. The expression $\theta = \sin^{-1} (\text{constant} + \sin \phi) \Big|_{f \text{ fixed}}$ is plotted for $-2 \leq \text{constant} \leq 2$.

As an example, the case of a known pattern for a main beam at 45° is indicated on the chart. Knowledge of that pattern completely defines all patterns within the region outlined by the dashed lines. One may note that even though some of these contours are not intersected by the known pattern, symmetry considerations allow extrapolation to a beam angle of -45° . It is not necessary that the array be symmetrical in spacing or weighting of elements for this principal to apply (this property is illustrated by Fig. 11, which is for an unevenly spaced array). Information about the portions of patterns farthest from the main beam is not obtained if the new main beam is farther from broadside than the initial main beam. Hence only part of the endfire pattern corresponding to the known pattern is obtained, as indicated by the dashed line at the top of the figure.

Fig. 13 - Contours of constant amplitude for any response pattern of a linear array with the beam formed at 90° . Normalized frequency is plotted vs signal arrival angle. Expression is $f/f_0 = \text{constant}/(\sin \phi - \sin \theta) |_{\theta = 90^\circ}$.



The frequency extrapolation chart shown in Fig. 13 is plotted for a beam angle θ of 90° . The corresponding endfire case is at the top of Fig. 12 and serves as the entry from the beam-angle extrapolation chart. Choice of the endfire case for communication between the two charts prevents loss of information in the transfer.

The chart of Fig. 13 covers a five-to-one frequency range. Choice of position on the frequency axis can be made to suit the direction of extrapolation desired. Information available will be limited to the contours extending over the signal-arrival-angle range of the known endfire pattern at the chosen frequency for entry to the chart. The portion of an endfire pattern obtained from the example in the previous plot, if entered at a normalized frequency of three, would define all patterns corresponding to the region within the dashed lines.

If a different beam angle were desired, the points for the new frequency would be returned to Fig. 12 for extrapolation. Choice of the endfire case for communication between the two charts prevents loss of information in the transfer.

The close resemblance of the extrapolation charts to plan views of the beam and frequency-dependence plots aids visualization of the extrapolation process. Complete information is preserved for lower frequencies and less oblique beam angles. The portion of the pattern near the main beam is obtained in other cases. In some cases, such as in going to a more oblique beam at a lower frequency, it is possible to regain in one chart the information lost in the other.

It is interesting to note that a portion of the directional response of an array could be determined by frequency-response measurements taken in a direction not coinciding with the main beam. In particular, if the main beam is formed in the endfire direction and frequency-response measurements are made in the opposite direction, a large portion of the directional response can be defined. The measured points would fall along the right edge of Fig. 13. They could then be followed along the curves to horizontal lines corresponding to directional response patterns. To include the main lobe, however, the frequency-response measurement would have to extend to zero frequency.

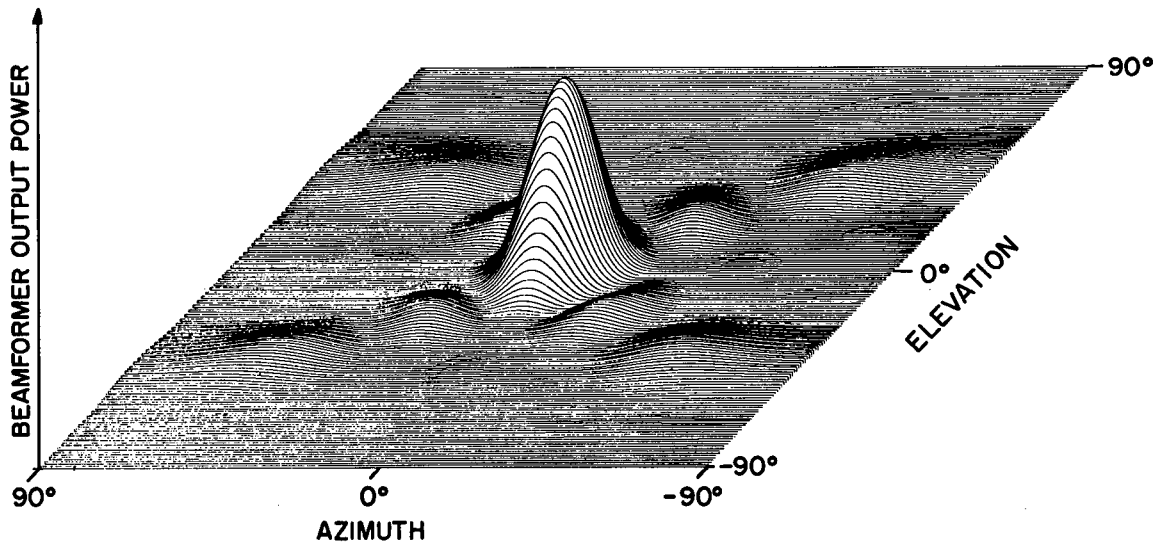


Fig. 14 - Beam is formed normal to a four-by-four, 16-element equispaced, unshaded, planar array. Array diagonals align with the horizontal and vertical axes. The response at frequency f_0 is shown in elevation and azimuth for an element spacing $\lambda \sqrt{2}/2$.

PLANAR AND VOLUME ARRAYS

The arrays examined thus far have been mainly linear arrays. Although linear arrays are the easiest type to construct, they provide directivity only in those planes which contain the array. At high frequencies it becomes practical to use planar and volume arrays.

Figure 14 shows the response in azimuth and elevation of a four-by-four, 16-element planar array. The main beam is formed broadside to the array. The third dimension in such a plot is used for the additional direction variable. Hence to show the dependence on an additional parameter, it would be necessary to choose some slice through the response surface as a starting point. It is more convenient in most cases to make a sequence of plots instead.

The array of Fig. 14 was oriented in the coordinate system with two of its corners at $\pm 90^\circ$ elevation. This did not show in the plot because the elements were approximately $1/2$ wavelength apart and only the main lobe had significant amplitude. Figure 15 shows the result of increasing the frequency by 50 percent. The central portion of this plot corresponds to the plot of Fig. 14. As the frequency becomes higher, these side lobes will move inward toward the center of the plot and be replaced by others coming in from the edges. Figure 16 shows the response at three times the original frequency. The array is now severely undersampled, and the side lobes show a periodic arrangement. The increased width of the more extreme side lobes arises from the smaller effective aperture presented to an oblique arrival, as in the linear array case.

The planar-array response shown in Fig. 16 was computed directly. Some computation time could have been saved, however, by the use of pattern multiplication. Detailed development and justification of the method is presented in Ref. 6. The principle can be applied by subdividing an array into like groups of sensors, each group having similar response patterns. This pattern is then multiplied times the pattern of a set of isotropic sensors having equivalent locations, relative amplitudes, and phases assigned to each of the individual groups. The technique is applicable whenever the expression for the response of the total array is equivalent to the product of two or more simpler factors. The method is particularly advantageous for determining the response of complex arrays or for synthesizing relatively complex patterns from known simple patterns. The technique is sufficiently

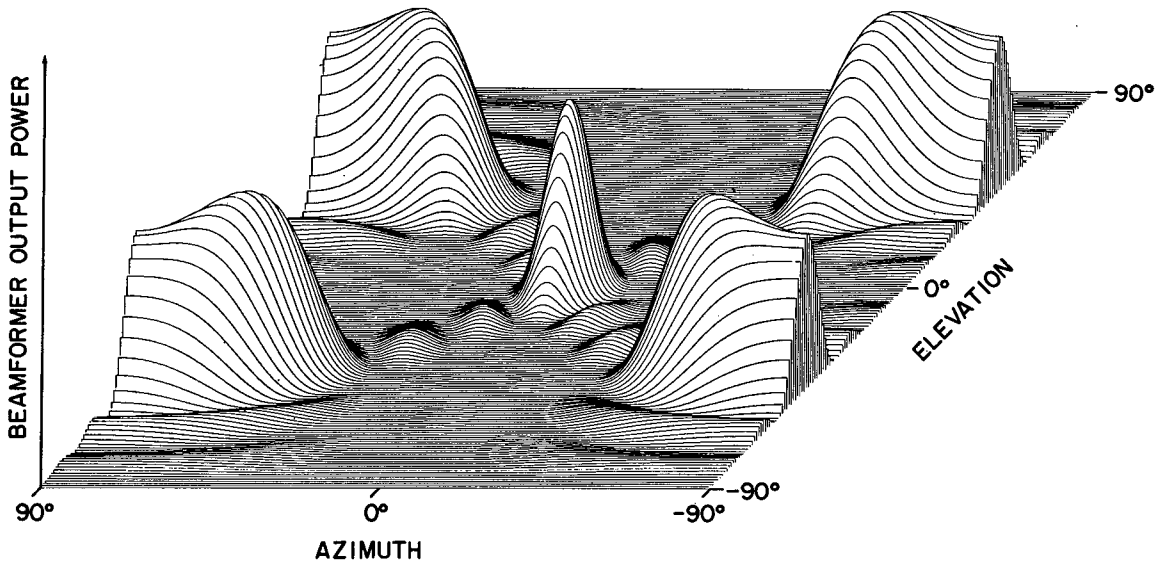


Fig. 15 - Response at $1.5 f_0$ of the same array as used for Fig. 14

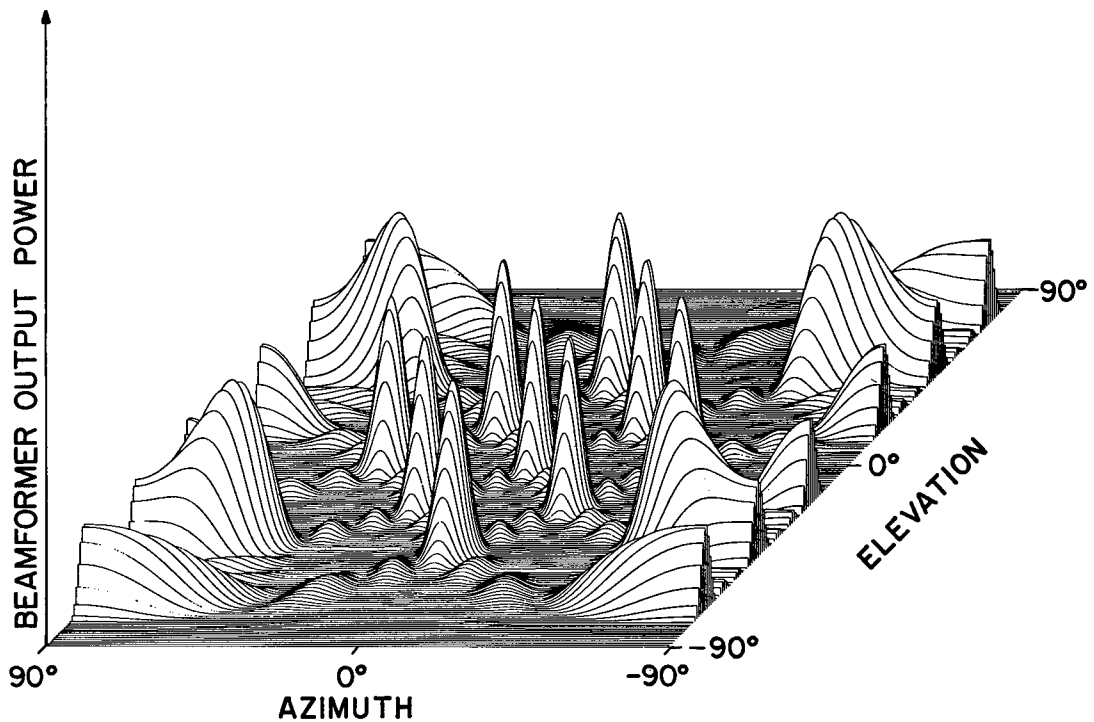


Fig. 16 - Response at $3 f_0$ of the same array as used for Fig. 14

useful that it is worthwhile to repeat the pattern computation of Fig. 16 by pattern multiplication with illustrative plots of the intermediate steps.

Figure 17 shows the 16-element planar array and two possible pairs of subarrays which could be used for pattern multiplication. The dimensions shown in wavelengths correspond to the frequency used for the plot of Fig. 16. The linear subarrays are the preferred choice, because their patterns will be mirror images of each other in elevation/azimuth coordinates. Hence only one pattern need be computed and stored. The required product can be obtained

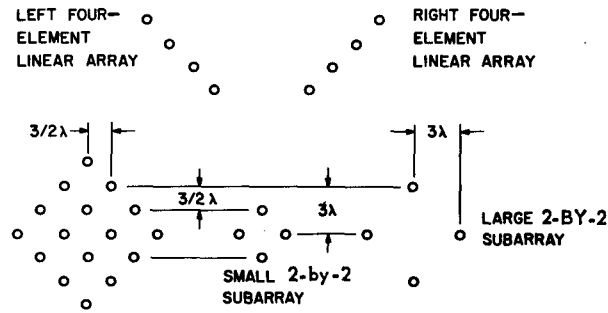


Fig. 17 - A 16-element array and two pairs of subarrays showing the possible choices for pattern multiplication. Dimensions correspond to the frequencies used for Fig. 16. The larger 2-by-2 subarray is spaced equivalent to the centers of four of the small 2-by-2 subarrays forming the 16-element configuration.

by taking successive multipliers and multiplicands from locations in the stored pattern, starting with values corresponding to opposite corners.

The patterns of the two linear subarrays are shown in Figs. 18 and 19. The mirror-image relationship is clearly visible. These patterns are figures of revolution with their respective arrays as axes. This is not obvious in the figures, because the use of elevation/azimuth coordinates is equivalent to projecting the patterns on the surface of a sphere. The product of these two patterns, point by point, is the pattern of Fig. 16. The contributions of the two individual patterns can be recognized more easily by looking at the underside of the pattern, as shown in Fig. 20. The lack of perspective correction in the plotting is quite a bit more conspicuous in the inverted plot, because the inverted base plane provides a frame of reference for the eye.

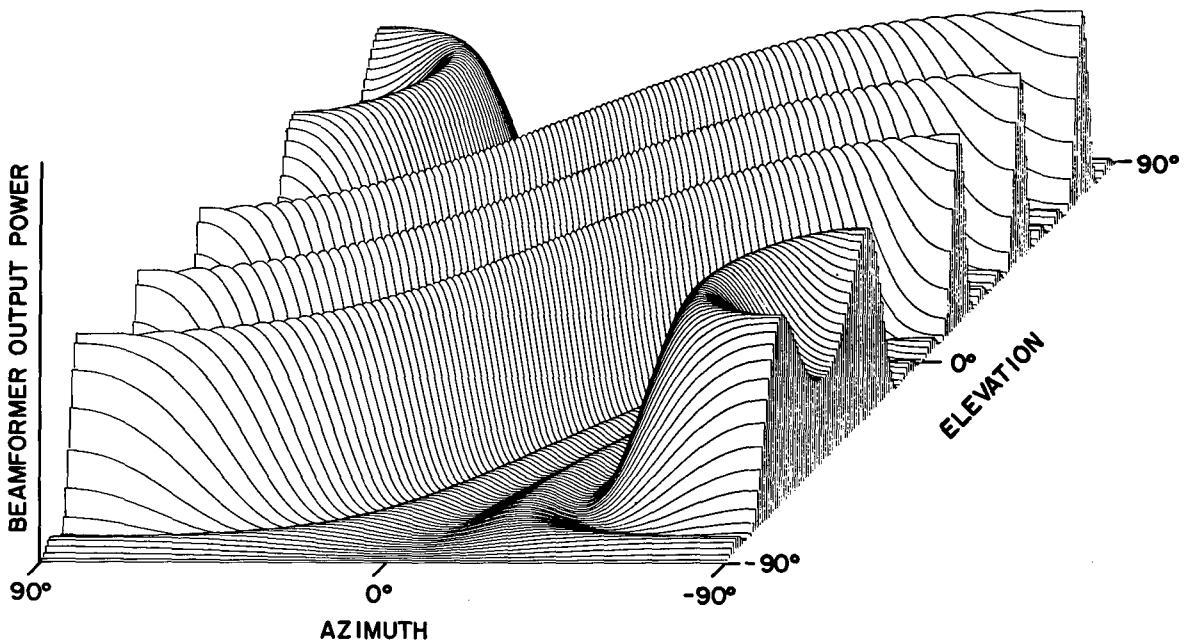


Fig. 18 - Elevation and azimuth response of the left four-element array of Fig. 17

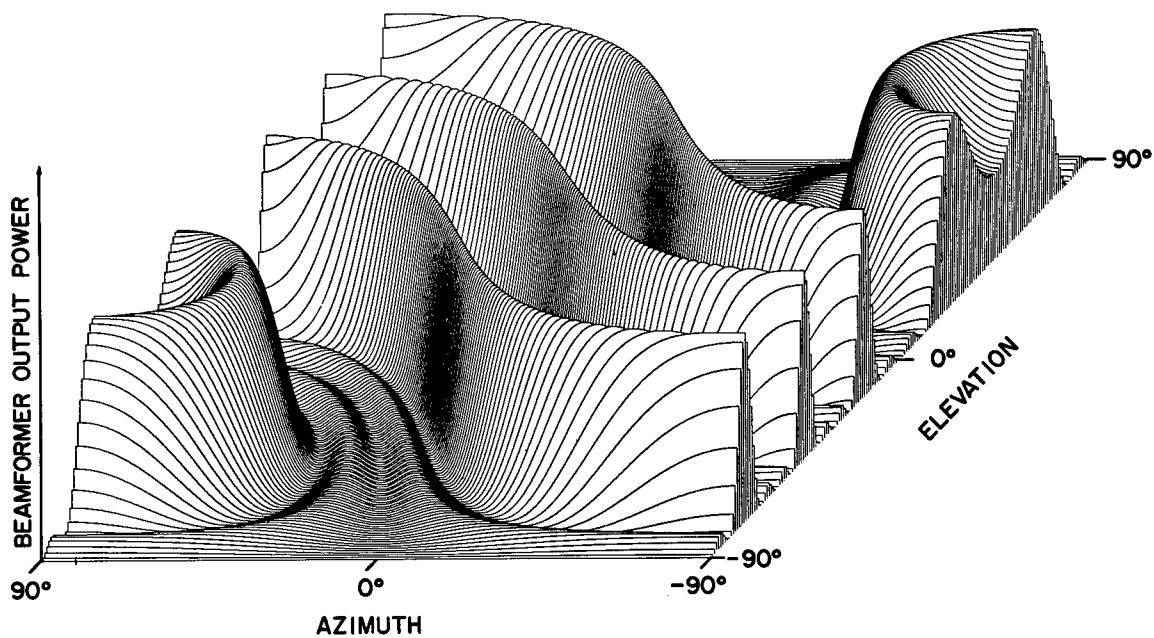


Fig. 19 - Elevation and azimuth response of the right four-element array of Fig. 17

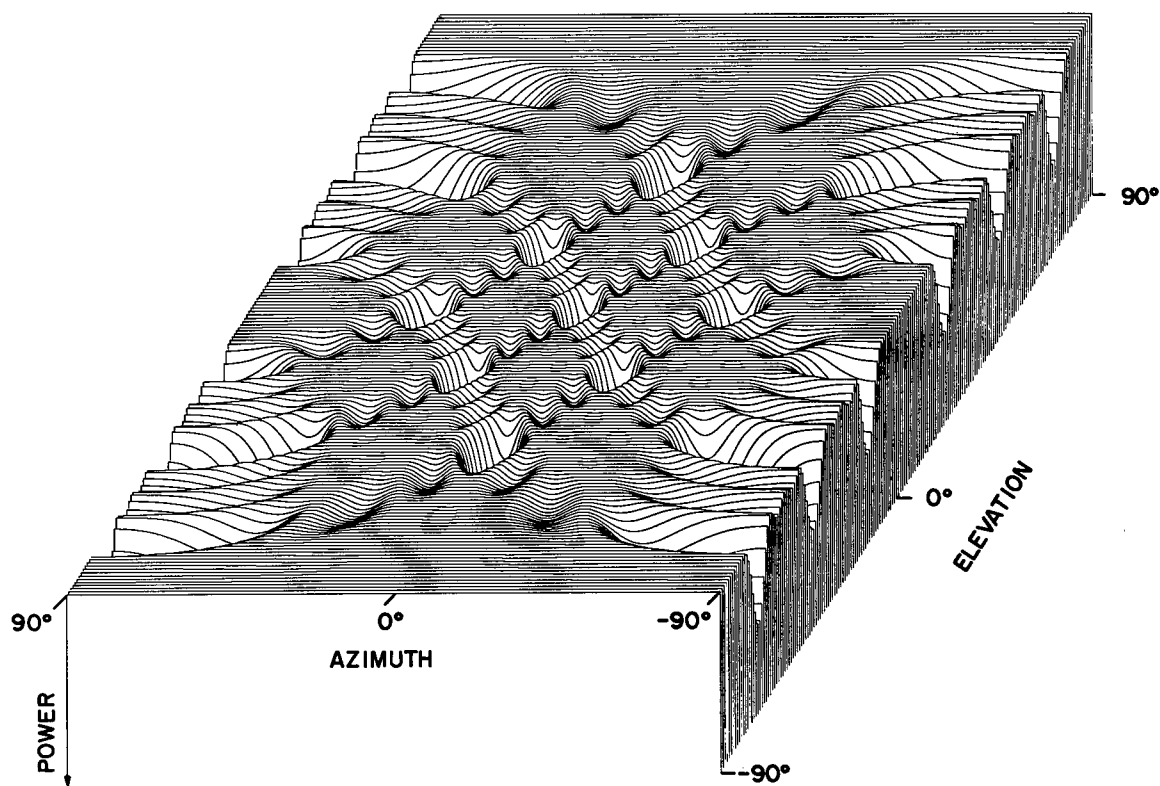


Fig. 20 - Response (inverted) obtained by pattern multiplication for the four-by-four planar array

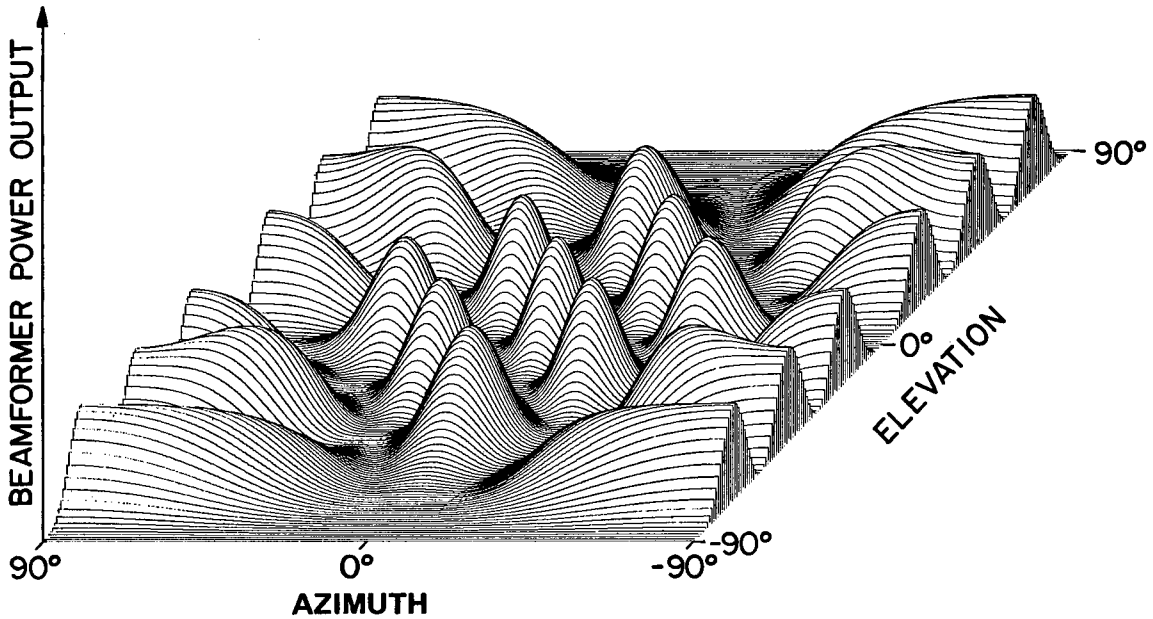


Fig. 21 - Response of the small two-by-two array of Fig. 17

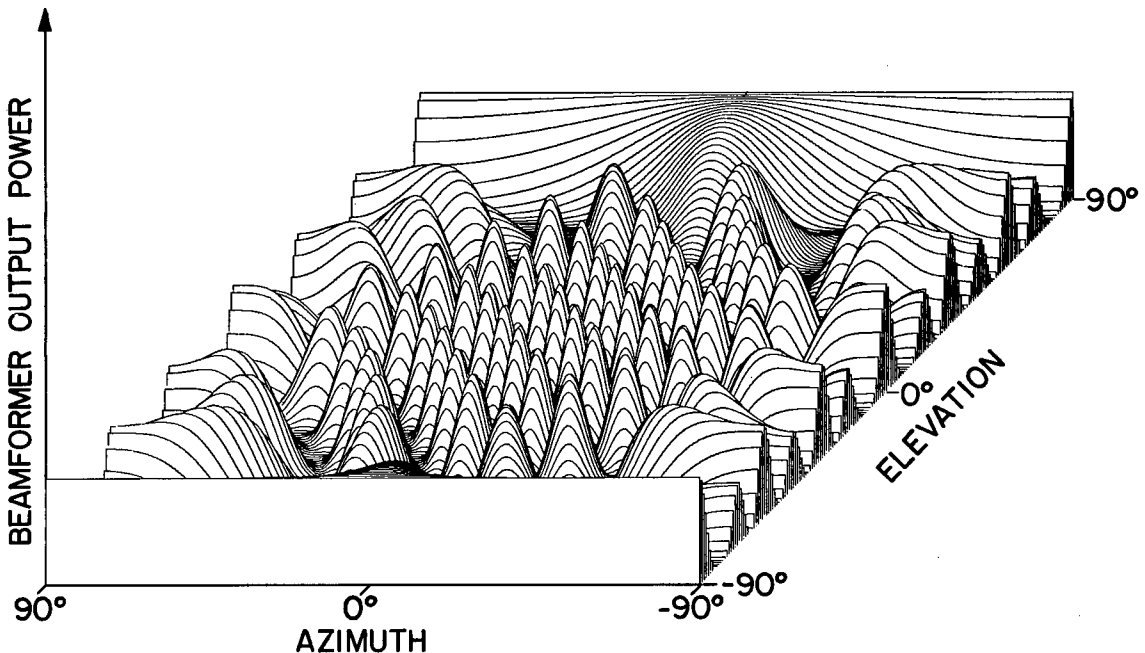


Fig. 22 - Response of the large two-by-two array of Fig. 17

The patterns of the other two possible subarrays are shown in Figs. 21 and 22. The small two-by-two array possesses the same symmetry and the same element spacing as the complete array. Hence its pattern is quite similar to that of the complete array, although broadened by the diffraction resulting from its smaller aperture. The larger two-by-two subarray is quite severely undersampled and hence has a large number of grating lobes. The lobes of the small array tend to select the lobes of the larger array visible in the resulting product pattern. The straight lines across the front and rear of the pattern of the

larger two-by-two array merely indicate the absence of nulls in the response at $\pm 90^\circ$ elevation.

The use of pattern multiplication is very advantageous for large arrays having a high degree of symmetry or periodicity. The process can be extended by factoring a large array into many small arrays. For a completely periodic array the gain in computational efficiency is similar to that which the fast Fourier transform affords over conventional techniques. This is to be expected, since the far-field pattern is a Fraunhofer diffraction pattern and hence is the Fourier transform of the element distribution.

The large number of elements in most volume arrays makes the use of pattern multiplication almost essential. The pattern of a four-by-four-by-four, 64-element volume array consisting of a stack of four of the arrays shown in Fig. 17 can be obtained by one additional pattern multiplication. Figure 23 shows the endfire pattern of a four-element linear array seen end-on in elevation/azimuth coordinates. The figure-of-revolution nature of a linear-array pattern is much more easily seen in this orientation. Multiplication of this pattern by the planar-array pattern of Fig. 16 results in the volume-array pattern of Fig. 24. The side-lobe selection effect of the multiplication is again quite evident.

USE OF COMPUTER PLOTS IN ARRAY STUDY

The examples in the previous section indicate the insight into array properties obtainable through the use of computer plotting techniques. Considerable care in the choice of parameters is required, however, to produce a meaningful and easy-to-interpret plot. One of the three available variables in a 3-D plot is used for the array response. Another is used for a parameter associated with signal arrival direction. These two quantities are essential in almost all array plots. The third variable can be selected from quantities such as frequency, amplitude-shading parameter, beam steering angle, and wavefront curvature or from an additional signal-arrival-direction parameter.

The orientation of a 3-D plot is quite important. The ridged surface obtained in frequency-response plots, such as Figs. 9 and 10, would be extremely difficult to interpret

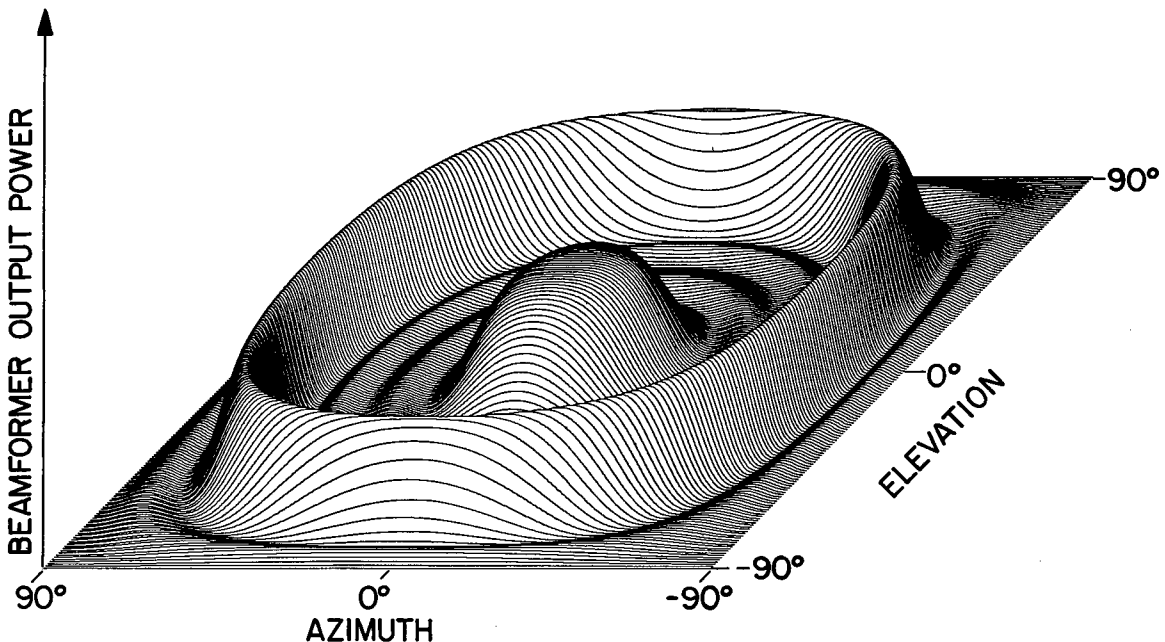


Fig. 23 - Endfire response of the four-element linear arrays of Fig. 17

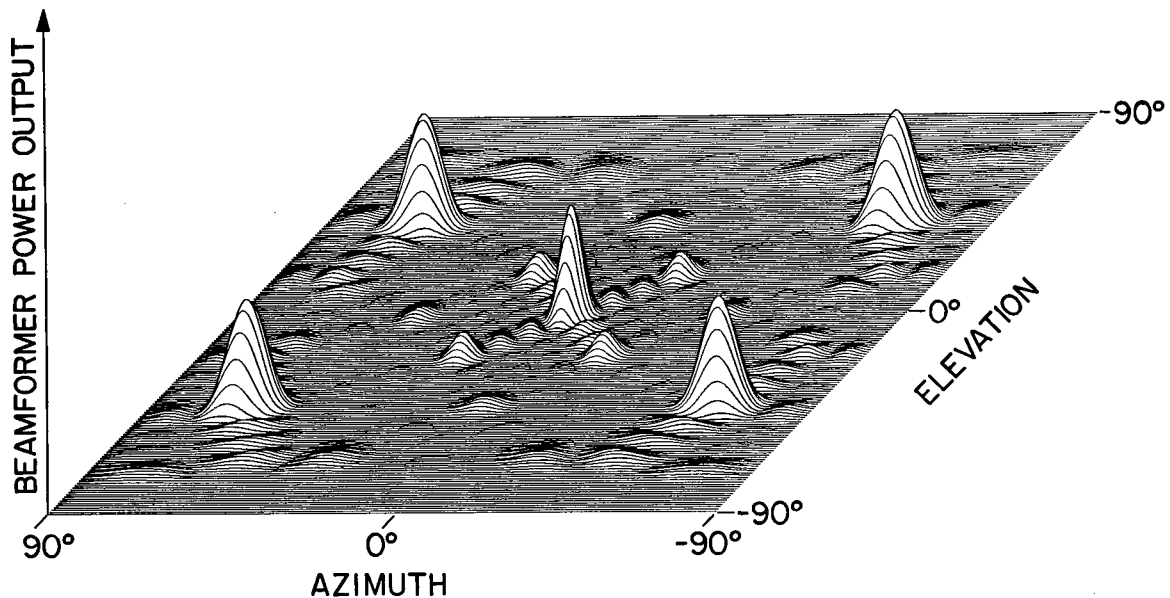


Fig. 24 - Response for a volume array resulting from multiplying the responses of Figs. 18, 19, and 23

if the axes used for signal arrival angle and frequency were interchanged. It would be quite difficult for the eye to separate individual ridges in the confusion of many lines almost parallel to the front of the plot.

It is also important that detail of interest in the center and rear of a plot not be hidden by higher features in the foreground. It is often advantageous to reverse the frequency axis and put the lower frequencies toward the rear of the plot if the response extends to extremely low frequencies. This prevents the very broad main lobe at low frequencies from hiding points farther back in the plot. The entire first line of an elevation/azimuth plot corresponds to a single direction, since the north and south poles of such a coordinate system are single valued in azimuth. If the array has a significant response in that direction, a straight line across the front of the plot will hide detail farther back. This effect is visible in Fig. 22. If the array had had a high side lobe in that direction, much of the first half of the plot would have been hidden. Choice of a different coordinate system or a slight change in the orientation or steering of the array to provide a null in that direction can be helpful.

Plotting a few selected slices of an array pattern is quite helpful in planning a 3-D plot. These can be used with the extrapolation charts of Figs. 12 and 13 to aid the choice of parameters.

Polar plots of array patterns are not adapted to 3-D use because of their inherently multivalued nature as seen in rectangular coordinates. They do possess the advantage of giving a direct feel for the relative directions of significant portions of the response. A power or amplitude plot in polar coordinates tends to be difficult to examine. Expansion of the origin by addition of a constant to all values cures this problem and also aids comparison with rectangular plots. The 1.5-kHz slice from Fig. 10 is shown in conventional and expanded polar plots in Fig. 25. The scale of both plots is the same.

The use of isometric presentations of array response have been valuable as a tutorial review and as an aid to insight into array properties. Observation of initial results led to further examination of the parameter relationships leading to the contour plots and their illustration of fundamental array properties. The computer programs continue in use for evaluation of specific array configurations and applications.

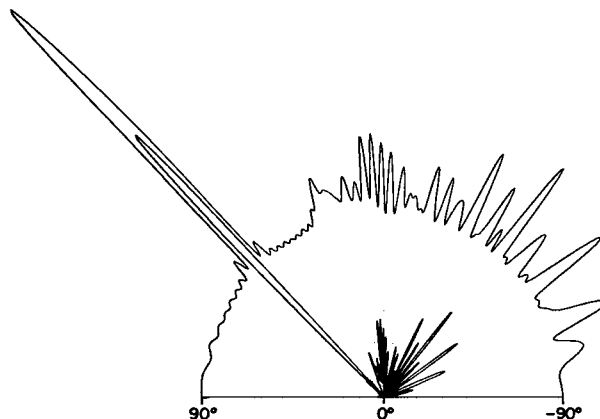


Fig. 25 - The expanded polar plot resulting from the addition of a constant to the values for the conventional plot

REFERENCES

1. J. Jenkins, "Program to Compute Array Response Surfaces," NRL Memorandum Report 2077, Sept. 1969
2. L.P. LaLumiere, "Hydrophone Array Power Response to a Spherical Wave," NRL Memorandum Report (in preparation)
3. L.P. LaLumiere, "Hydrophone Array Power Response to a Plane Wave," NRL Memorandum Report (in preparation)
4. P. Jacquinot and B. Roizen-Dossier, "Apodization" in *Progress in Optics* Vol. III, E. Wolf, Ed., pp. 29-186, John Wiley and Sons, New York, 1964
5. J.D. Kraus, *Antennas*, McGraw-Hill, New York, 1950, pp. 97-109
6. J.D. Kraus, *Antennas*, McGraw-Hill, New York, 1950, pp. 66-74

(Related references not cited in text)

7. J.V. DiFranco and W.L. Rubin, "Spatial Ambiguity and Resolution for Array Antenna Systems," *IEEE Transactions on Military Electronics MIL-9*, (1965)
8. A. Friedman, "Distortion in Acoustic Beams Steered by Means of Continuous Phase Taper," U.D.E. Pamphlet No. 643, 1959 (Curves of beam width versus beam steering angle are presented which contain information equivalent to the beam extrapolation curves of Fig. 13)
9. G.V. Olds, "Incremental Plotting Techniques in 3-D" (summary of plotting technique), NRL Report (in preparation)

DOCUMENT CONTROL DATA - R & D

(Security classification of title, body of abstract and indexing annotation must be entered when the overall report is classified)

1. ORIGINATING ACTIVITY (Corporate author) Naval Research Laboratory Washington, D.C. 20390		2a. REPORT SECURITY CLASSIFICATION Unclassified	
		2b. GROUP	
3. REPORT TITLE ARRAY BEAMFORMING RESPONSE STUDIES			
4. DESCRIPTIVE NOTES (Type of report and inclusive dates) An interim report on one phase of the problem.			
5. AUTHOR(S) (First name, middle initial, last name) George W. Byram, George V. Olds, and Leon P. LaLumiere			
6. REPORT DATE October 14, 1971		7a. TOTAL NO. OF PAGES 24	7b. NO. OF REFS 9
8a. CONTRACT OR GRANT NO. NRL Problem S01-39		9a. ORIGINATOR'S REPORT NUMBER(S) NRL Report 7331	
b. PROJECT NO. RF 05-552-403-4069		9b. OTHER REPORT NO(S) (Any other numbers that may be assigned this report)	
c.			
d.			
10. DISTRIBUTION STATEMENT Approved for public release; distribution unlimited.			
11. SUPPLEMENTARY NOTES		12. SPONSORING MILITARY ACTIVITY Department of the Navy Office of Naval Research Arlington, Virginia 22217	
13. ABSTRACT Computer graphics have been used to display the results of array beamformer computations in a form aiding insight into beamforming characteristics. In particular, the effect of a parameter such as frequency, wavefront curvature, beam angle, or shading on array response can be easily seen. The examples are chosen to illustrate those characteristics as well as to aid insight into a number of important array properties. The associated theory is briefly summarized with each example, and the emphasis on important array properties makes the report useful as a tutorial review.			

UNCLASSIFIED

14. KEY WORDS	LINK A		LINK B		LINK C	
	ROLE	WT	ROLE	WT	ROLE	WT
Array beamforming Linear array Planar array Volume array Array focusing Array shading Array pattern extrapolation Pattern multiplication Computer isometric displays						